Silicon (2022) 14:6291–6297
https://doi.org/10.1007/s12633-021-01403-x

ORIGINAL PAPER

Manufacturing Porous Materials Using Dabco-Based Ionic Liquid

Haleh Sanaeishoar[1] · Maryam Sabbaghan[2] · Maryam Ghazvini[3] · Maryam Ghanbari[2] · Sahar Peimanfar[1]

Received: 16 February 2021 / Accepted: 16 September 2021 / Published online: 1 October 2021

Abstract

The long-chain ionic liquid (IL) hexadecyl-4-aza-1-azoniabicyclo[2.2.2]octane bromide was used as a template to prepare the hexagonally ordered siliceous mesoporous molecular sieve MCM-41 as well as the disordered mesoporous molecular sieve designated as KIT-1. The synthesized products were studied via X-ray diffraction (XRD), Fourier transform infrared (FTIR), N_2 adsorption-desorption analysis, scanning electron microscopy (SEM) and transmission electron microscopy (TEM). Also, the surface area (BET), pore volume, and pore diameter (BJH) are determined. These kind of ILs which have 1,4-diazabicyclo[2.2.2]octane (DABCO) in their structures, were prepared with an easy method. When the two templates, cetyltrimethylammonium bromide (CTAB) and IL, have the similar structures, MCM-41 mesoporous molecular sieve produced with more ordered, uniform mesoporous channel and high surface area in comparison to without IL. When just IL used instead of CTAB, the KIT-1 with non-uniform mesoporous was obtained. Here we prepared the KIT-1 mesoporous molecular sieve with IL without CTAB. Also, using dual template CTAB and DABCO based IL leads to increase the pore walls of products. It seems, using dual template with changing IL structures in fabricated of molecular sieve provide new opportunity to design targeted adsorbents and catalysis.

Keywords MCM-41 · KIT-1 · CTAB · DABCO-based long chain ionic liquid

1 Introduction

Over the last two decades, the preparation of high surface area mesoporous materials has captured great interest within the scientific community. Much attention has been given lately to various mesoporous silica materials, such as M41S, KIT-1, and SBA-15 [1–3]. These structurally well-defined materials have promising utilizations in catalysis, separation, adsorption, sensing, and delivery of drugs [4, 5]. In 1992, mesoporous molecular sieves M41S were discovered by Mobil staff. This outstanding finding has provoked substantial research in this area. One of the most noteworthy mesoporous molecular sieves to mention is MCM-41 which has a hexagonal array of uniform mesoporous [1]. In order to improve preparatory process, some novel templates were employed in our previous work [6].

KIT-1 is a noncrystalline molecular sieve that displays short worm-like channels. The channels are organized in a disordered three-dimensional system with numerous seams. The channel widths, however, are as uniform as those in the well-ordered mesoporous molecular sieves, MCM-41 [2]. The hydrothermal stability of KIT-I is higher than that of the ordered MCM-41 [7]. This kind of molecular sieve reduces probability of channel blockage in its catalytic activity.

There has been much research in recent years into the synthesis methods of MCM-41, [8–11] but only a few studies have been carried on the synthesis methods of KIT-1. One of these studies was conducted in 1996 by Ryoo et al., and it successfully synthesized KIT-I, for the first time, by an electrostatic templating route by means of ethylenediaminetetraacetic acid tetrasodium salt ($EDTANa_4$), hexadecyltrimethylammonium chloride (HTACl), and sodium silicate [2]. Another study was done in 1997 by Ryoo et al. which established another approach to the synthesis of KIT-1 [12]. Synthesis of KIT-1 has been achieved, in the presence of different polyacids, by hydrothermal

✉ Haleh Sanaeishoar
hsanaei@iauahvaz.ac.ir

✉ Maryam Sabbaghan
sabbaghan@sru.ac.ir; msaba16us@yahoo.com

[1] Department of Chemistry, Ahvaz Branch, Islamic Azad University, Ahvaz, Iran

[2] Chemistry Department, Faculty of Sciences, Shahid Rajaee Teacher Training University, PO Box 16785-163, Tehran, Iran

[3] Department of Chemistry, Payame Noor University, Tehran, Iran

Scheme 1 Chemical structure of CTAB, [C_{16}dabco]Br (**IL-C_{16}**), [C_{12}dabco]Br (**IL-C_{12}**), [C_4dabco]Br (**IL-C_4**)

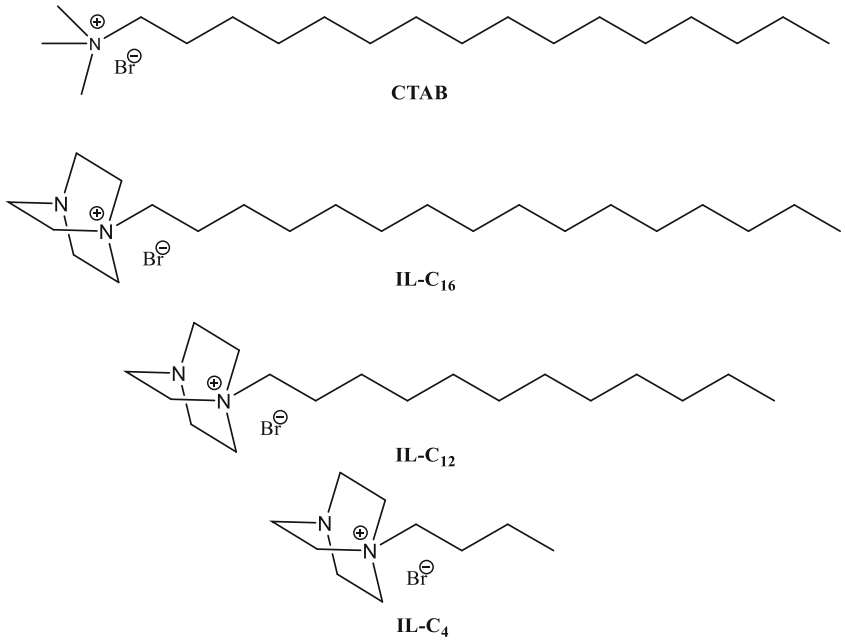

polymerization of silicate anions surrounding the molecular organization of hexadecyltrimethylammonium chloride [12].

Ionic liquids (ILs), organic salts with low melting points, have been extensively examined and have exceptional characteristics such as extreme stability, high ionic conductivity, non-volatility, adjustable polarity, and recyclability [13, 14]. Lately, ILs have been the focus of noticeable consideration not only in chemistry but also in materials science [13]. Specific self-assembled structures can be created with the opportunity of adjustment the amphiphilicity of ILs by modifying the polarizability of the anion and cation or the alkyl chain length. Some researchers in the domain of sustainable green synthesis have paid considerable attention to ILs during the last few decades [15]. ILs were used as a template or solvent, in green chemistry, for nanomaterial synthesis [10, 13].

There has been no work in the publications that reports the use of long chain IL based DABCO for mesoporous system synthesis. In the present work, the new IL, hexyldecyl-4-aza-1-azaniabicyclo[2.2.2]octane (**IL-C_{16}**) was synthesized. Structure of used IL is shown in Scheme 1. This structure in compared with CTAB structure is the same long chain and the anion (Scheme 1). The question arises what effect has similarity between CTAB and IL structures used on the mesoporous structure?

In connection with our interest in influence of different ILs as co-template in micro-mesoporous MCM-41 structure and disordered mesoporous material KIT-1, here, we report the results of a study on the **IL-C_{16}** with similar structure with CTAB as dual template (**MCM-41–1**) and absence of CTAB (**KIT-1-1**). Also, the results were compared with **MCM-41–2** as reference sample and **KIT-1-2** materials from our previous article [16]. In preparation of **MCM-41–2** was used only CTAB as template and **KIT-1-2** was used dual template CTAB and dodecyl-4-aza-1-azaniabicyclo[2.2.2]octane (**IL-C_{12}**). The other ILs used in this research were [C_{12}Dabco]Br (**IL-C_{12}**) and N-butyl-4-aza-1-azaniabicyclo[2.2.2]octane bromide abbreviated [N-buDabco]Br (**IL-C_4**) (Scheme 1). The detailed synthesis conditions are shown in Table 1.

Table 1 The corresponding experimental conditions and structural parameters of the micro-mesoporous silicates

Sample	IL	SiO_2:CTAB:IL	d_{100} (nm)	a_0 (nm)	D_p (nm)	W_t (nm)	S_{BET} (m^2g^{-1})	V_{tot} (cm^3g^{-1})
MCM-41–1	C16[b]	1:0.2:0.2	3.74	4.32	2.42	1.90	1221	0.68
MCM-41–2[a]	–	1:0.4:0	3.83	4.22	2.42	1.80	1028	1.03
KIT-1-1	C16[b]	1:0:0.4	3.47	4.00	2.42	1.58	524	0.55
KIT-1-2[a]	C12[c]	1:0.2:0.2	4.01	4.63	2.42	2.21	1012	1.12

[a] Synthesis method and characterization of this sample were reported in Ref. 16

[b] The same alkyl side chain length with CTAB

[c] The same molecular weight with CTAB

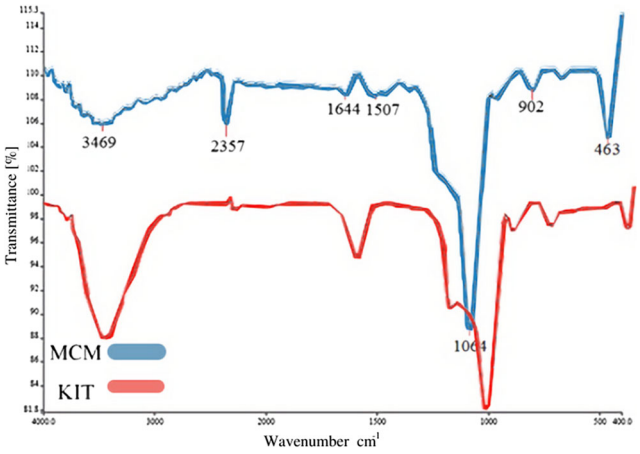

Fig. 1 FT-IR spectra for **MCM-41–1** and **KIT-1-1**

2 Experimental

2.1 Characterization

All the reagents were obtained from Merck or Aldrich and were used without further purifications. ^{1}H NMR spectra were recorded on a Bruker DRX-250 (250 MHz) spectrometer in $CDCl_3$. Carbon nuclear magnetic resonance (^{13}C NMR) spectra were recorded on a Bruker DRX-250 (62.9 MHz). The crystalline structures of the resultant samples were characterized by X-ray diffractometer (XRD, X'Pert Pro MPD, PANalytical) with Cu Kα radiation (40 kV and 40 mA). The FT-IR spectra were recorded using a Perkin-Elmer BX-II IR spectrometer. N_2 adsorption/desorption isotherms of samples were made at 77 K (BELSORP-mini II, MicrotracBEL, Corp.), the degas temperature was 250 °C. The specific surface area and mesopore size distribution were determined by BET and BJH (Barrett–Joyner–Halenda) method, respectively [17]. Morphology of the samples were characterized by scanning electron microscope (SEM, SCAN MIRA3-XMU) with an acceleration voltage of 0.2–30 kV. Transmission electron microscopy (TEM) was performed by Philips CM300.

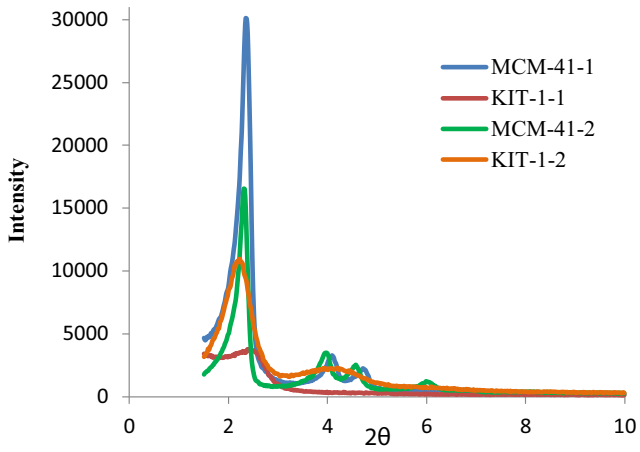

Fig. 2 XRD for the **MCM-41–1**, **MCM-41–2**, **KIT-1-1** and **KIT-1-2**

2.2 Ionic Liquid Preparation

2.2.1 Hexadecyl-4-Aza-1-Azoniabicyclo[2.2.2]Octane Bromide (IL-C_{16})

To 17.8 mmol DABCO (98% Pure) in 50 mL AcOEt, 18.7 mmol 1-bromohexadecan was added, and the mixture was stirred at room temperature (r.t.) for 24 h. Then the solvent was removed by rotary evaporator. Then the product was suspended into diethyl ether (30 cc) and stirred for 1 h at r.t. The product was filtered and dried in vacuum to give the title compound (6.7 g, 90%).

^{1}H NMR ($CDCl_3$, 250 MHz,): δ = 0.80 (t, 3H, J = 6.75 Hz), 1.12–1.25 (m, 26H), 1.67–1.71 (m, 2H), 3.19 (t, 6H, J = 7.0 Hz), 3.36–3.42 (m, 2H), 3.60 (t, 6H, J = 7.5 Hz). ^{13}C NMR ($CDCl_3$, 62.9 MHz): δ = 13.99, 22.02, 22.52, 26.31, 29.09, 29.17, 29.31, 29.45, 31.74, 45.30, 52.37, 64.51.

2.2.2 Preparation of MCM-41–1

In a typical synthesis, Ethylamine was used to control the pH value of the aqueous solution (pH =12), and CTAB and **IL-C_{16}** were used as a dual template. The needed quantity of TEOS was added drop-wise to the mixture. The mixed gel had the following molar constitutions: (SiO_2:CTAB:IL:EA:H_2O) = (1:0.2:0.2:0.6:100). After the TEOS was added, the solution was mixed-up firmly for 2 h at r.t. The mixture was then moved into a stainless-steel autoclave and exposed to a high temperature at 373 K for 48 h. The resultant product was washed with EtOH one time and then two times with deionized water. Then it was left to dry at 373 K to get the product. The as-synthesized sample was then left in the air to get calcined for 6 h at a temperature of 823 K and a heating rate of 1 K min^{-1}.

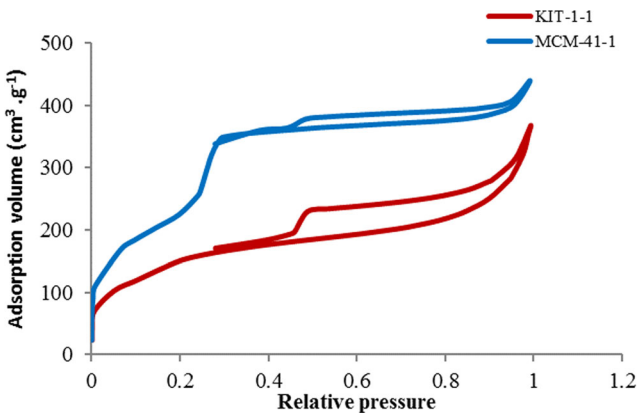

Fig. 3 N_2 adsorption-desorption isotherm curves of the synthesized solids

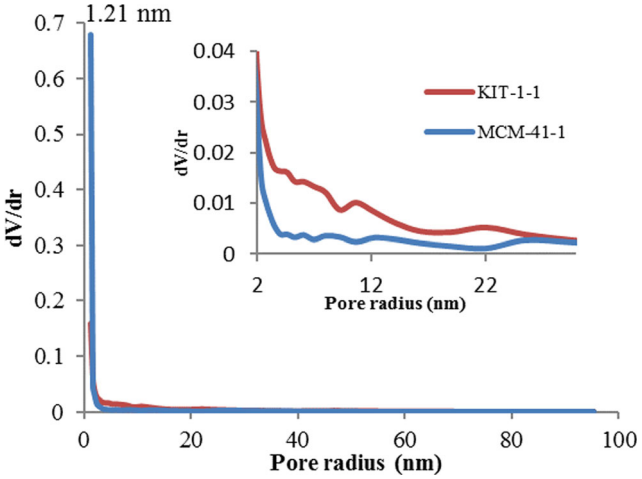

Fig. 4 Pore size distribution (radius) for synthesized solids calculated by BJH method

2.2.3 Preparation of KIT-1-1

In a typical synthesis, Ethylamine was used to control the pH value of the aqueous solution (pH = 12). The needed quantity of TEOS was added drop-wise to the solution. The mixed gel had the following molar constitutions: (SiO_2:IL:EA:H_2O) = (1:0.4:0.6:100). After the TEOS was added, the solution was mixed-up firmly for 2 h at room temperature. The mixture was then moved into a stainless-steel autoclave and exposed to the temperature of 373 K for 48 h. The resultant product was washed one time with EtOH and two times with deionized water. Then it was left to dry at 373 K to get as-synthesized sample. The as-synthesized sample was then left in air to get calcined for 6 h at a temperature of 823 K and a heating rate of 1 K min^{-1}.

2.2.4 Preparation of MCM-41–2 and KIT-1-2

MCM-41–2 and **KIT-1-2** were prepared based on our previous work [16].

3 Results and Discussion

Figure 1 illustrates the IR spectra of **KIT-1-1** and **MCM-41–1** materials. The bending modes of Si–O–Si bands are believed to cause the signals at 463–467 cm^{-1}. The symmetric/asymmetric stretching vibrations of Si-O-Si bonds are thought to lead to the bands at 799–804 cm^{-1} and 1064–1078 cm^{-1}, respectively. The asymmetric vibrations of (Si–OH) are presumably generating the signals at 953–965 cm^{-1}.The bending and stretching modes of adsorbed water molecules are believed to account for and contribute to the bands at 1640–1644 cm^{-1} and 3460–3465 cm^{-1}.

The small-angle XRD patterns of the products are shown in Fig. 2. XRD patterns of **MCM-41–1** indicated an intense sharp (100) peak, followed by minor (110) and (200) peaks, matching to a highly ordered hexagonal structure of MCM-41. XRD patterns confirm that by using dual templates, CTAB and IL, the crystallization of **MCM-41–1** increased in comparing with **MCM-41–2**. The (100) peak of **MCM-41–1** shift toward the slightly bigger angle, which shows the lattice space d_{100} of the pores ($d_{100} = \lambda/2\sin\theta$) became smaller. On the other hand, the low intensity and peak broadening detected in the XRD pattern of **KIT-1-1** and **KIT-1-2** indicate that these materials are not as well ordered as MCM- 41 and the structure array of their channels is disorder [18]. Two wide peaks which correspond to (100) and (200) diffraction in XRD pattern for **KIT-1-1** showed a more disordered structure than **KIT-1-2**. As the Fig. 2 showed, using the dual templates to

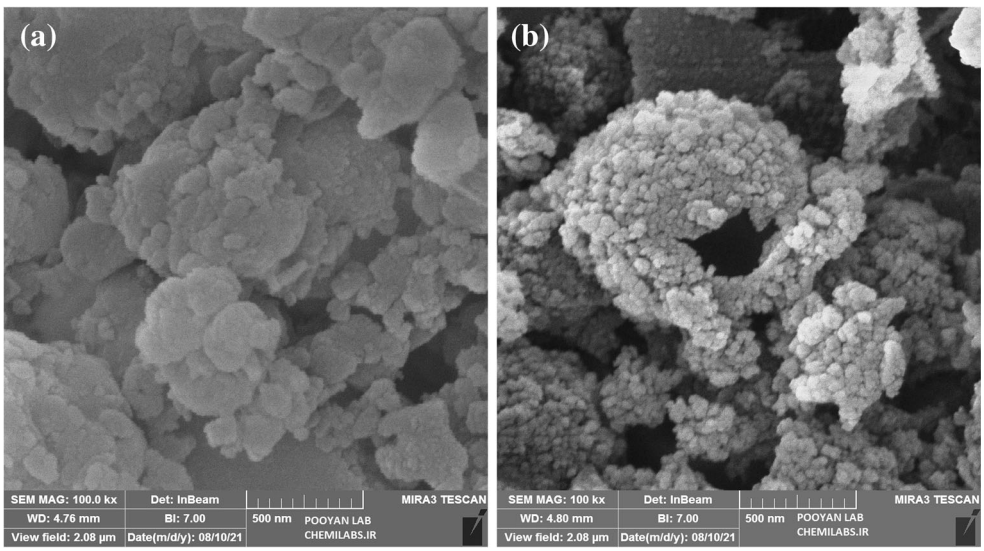

Fig. 5 SEM images of the **MCM-41–1** (a) and **KIT-1-1** (b)

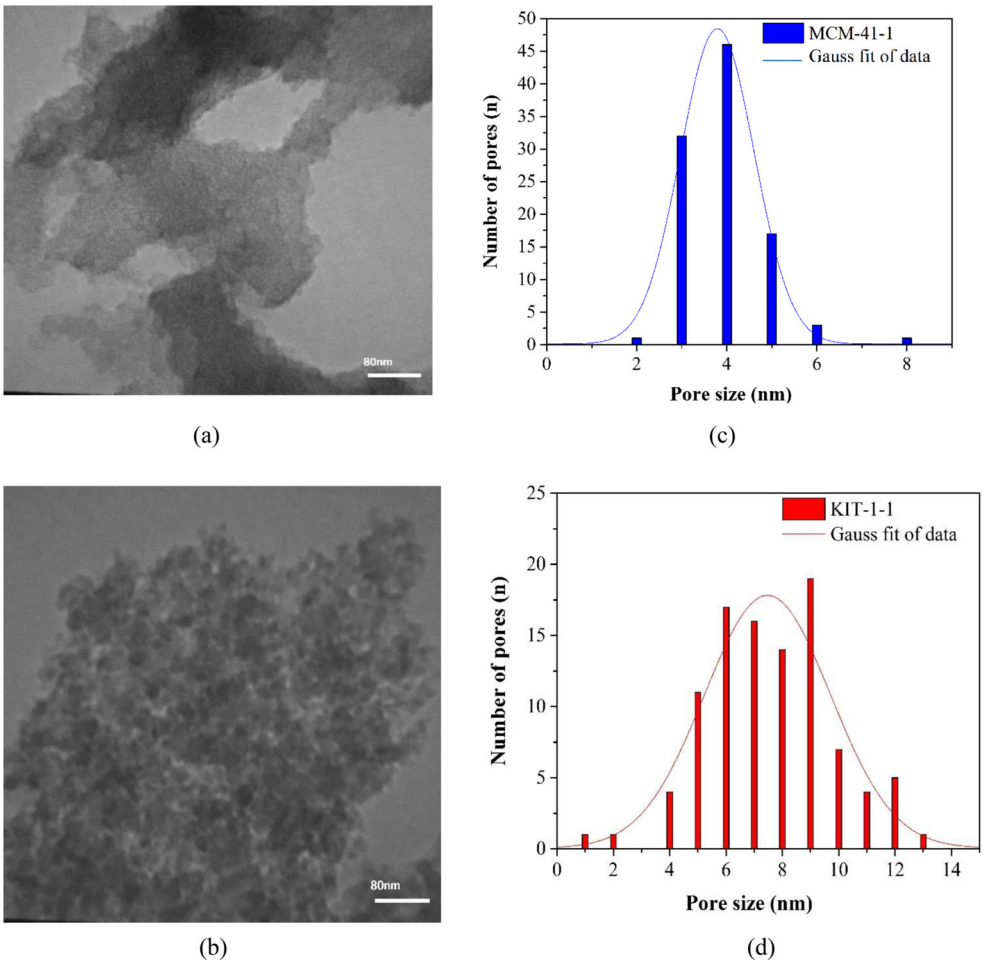

Fig. 6 TEM images of the **MCM-41–1** (a), **KIT-1-1** (b), the histogram of the pore size distribution of the **MCM-41–1** (c) and **KIT-1-1** (d)

produce **MCM-41–1** and **KIT-1-2** (Table 1, Entry 1 and 4) more ordered in comparing with one template (Table 1, Entry 2 and 3). The d_{100} spacing and calculated crystal lattice parameter ($a_o = 2d_{100}/\sqrt{3}$) of the samples are increasing in the following pattern: **KIT-1-2** > **MCM-41–1** > **MCM-41–2** > **KIT-1-1** (Table 1). The lattice increment may be

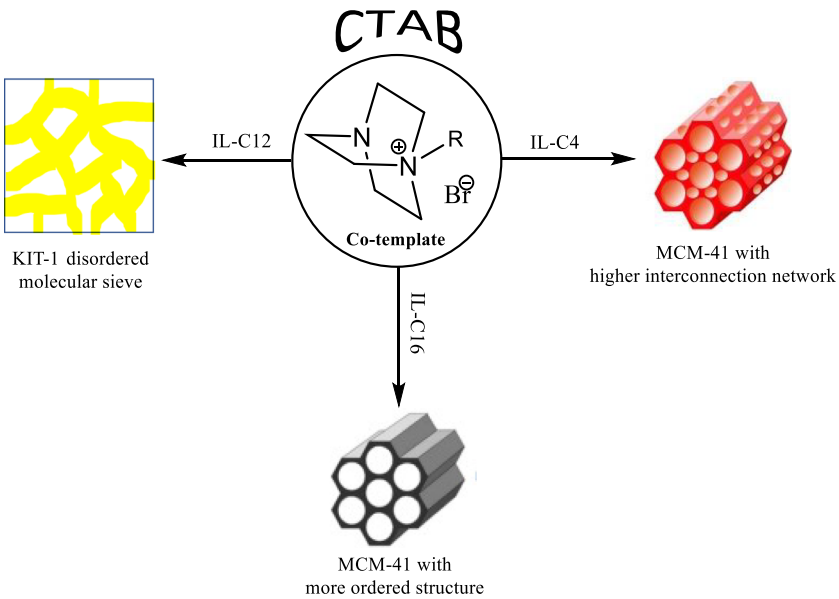

Scheme 2 Comparing the present research with our previous papers about role of IL based on DABCO in micro-mesoporous systems

attributed to the increasing of the pore walls of porous materials, which became more condensed with addition of DABCO based ILs along with CTAB in the synthesis system.

Nitrogen adsorption/desorption isotherms of samples show the typical type IV isotherm according to the IUPAC nomenclature for mesoporous structure (Fig. 3). The sharp inflection at P/P_0 = 0.3–0.35 in the isotherms of **MCM-41–1** sample indicates the narrow uniform mesoporous distribution. The existence of hysteresis loops in the **MCM-41–1** sample illustrates interaction network of porous structure which may be correlated to the existence of micropores, but **KIT-1-1** shows bigger hysteresis loop corresponds to the three-dimensional interconnection structure [19]. The sharp inflection p/p_0 in the isotherm **KIT-1-2** indicates the narrow uniform mesoporous distribution in comparing with **KIT-1-1** (Fig. SD. 3) [16].

Table 1 summarizes surface area and the pore volume of the characteristic MCM-41 and KIT-1 samples. The BET surface area, total pore volume and mean pore diameter (D_p) obtained from the nitrogen sorption. Wall thickness (W_t) values was calculated using $W_t = a_o - D_p$.

The BET surface area of **MCM-41–1** is 1221 m^2g^{-1}, which is bigger than the value of 1028 m^2g^{-1} for **MCM-41–2** but BET surface area of **KIT-1-2** is 1012 m^2g^{-1}, which is bigger than about twice the value of 524 m^2g^{-1} for **KIT-1-1**. The specific surface area of the **KIT-1-2** is upper 1000 $m^2\ g^{-1}$ and is also near to the ordered MCM-41.

The pore volume of **MCM-41–1** is 0.68 cm^3g^{-1}, which is smaller than the value of 1.03 cm^3g^{-1} for **MCM-41–2** and the pore volume of **KIT-1-1** is 0.55 cm^3g^{-1}, which is smaller than about half the value of 1.12 cm^3g^{-1} for **KIT-1-2**.

The pore size distribution of the mesopore and micropore of the products was obtained from desorption data using the BJH method (Fig. 4). **KIT-1-1** Sample shows non-uniform channels with 4–25 nm radiuses in comparison to **MCM-41–1**. Fig. SD.4. shows the TEM micrograph of **KIT-1-2** sample. It presents that the pore structure is the disorder network of short wormlike channel of mesoporous. These channels are connecting in a three dimensional with uniform pore size [26]. Also, the results confirm the ordered structure of **MCM-41–1** in comparing with the **MCM-41–2** and the **KIT-1-2** in comparing with the **KIT-1-1**.

The morphology of **MCM-41–1** and **KIT-1-1** samples was investigated using SEM technique. Figure 5 shows these samples result coral-liked structure. Figure 6a, b shows the TEM images of **MCM-41–1** and **KIT-1-1** samples. **MCM-41–1** and **KIT-1-1** exhibit a worm-like structure with a disorganized porous network. It should be noted that complex interactions between different kinds of surfactants can affect the pore ordering and lead to disorganized structures [20, 21]. In order to obtain the pore size distribution [22] from TEM images, the Digimizer version 5.4.6 software was used. The histogram of the pore size distribution was obtained by measuring about 100 pores in arbitrarily chosen areas in Digimizer. The pore size distribution reveal that the **MCM-41–1** provides the pore size distribution about 4 nm. While, the **KIT-1-1** sample is centered at 9 nm and 6 nm (see Fig. 6c,d).

It seems that **IL-C_{16}** role is the formation of ordered micelles with CTAB. Using only **IL-C_{16}**, with steric hindrance in cationic center, leads to formation of micelles that does not have good interaction with silicate polyanion in the polymerization process.

Wang et al. reported to investigation of 1-hexadecyl-3-methylimidazolium chloride (C_{16}mimCl) as a template, without CTAB, on synthesis of mesoporous silica in which the molar compositions of the mixed gel were: 1 TEOS: 0.543 C_{16}mimCl: 0.512 NaOH: 56 H_2O led to MCM-48 structure [23]. As we mentioned here using only [C_{16}Dabco]Br without CTAB provide the disordered mesoporous system as KIT-1.

In continuing our previous researches [6, 16], three cationic ILs based on DABCO with different chain length were applied as co-templates along with CTAB to produce micro-mesoporous silica materials. The using **IL-C_4** as co-template, showed good impact to prepare MCM-41 with higher interconnection network than using just CTAB [6]. The **IL-C_{12}** with the same molecular weight with CTAB caused to form the KIT-1 micro-mesoporous system [16]. The **IL-C_{16}** with the similar to CTAB structure in the length of the alkyl side chain leads to produce the micro-mesoporous MCM-41 with more order structure than comparison with only using CTAB (the present work). All of the synthesized mesoporous material has high surface area (Scheme 2).

4 Conclusion

In conclusion, using DABCO based IL with different chain as co-template along with CTAB take advantages in manufacturing porous materials like increasing interconnections, more ordered structure of mesoporous or preparation of disordered channel (KIT-1). Preparation of KIT-1 by only DABCO based IL with similar structure with CTAB as template leads less order in comparing with dual template. Moreover, crystal lattice parameter and wall thickness of products increase in dual template synthesis. This work has completed the results of previous works about the effect of DABCO based ionic liquid for synthesis porous materials.

Supplementary Information The online version contains supplementary material available at https://doi.org/10.1007/s12633-021-01403-x.

Acknowledgements The authors wish to thank the Ahvaz Branch, Islamic Azad University for providing the essential financial support.

Availability of Data and Materials Not applicable.

Author Contributions HS: Conceptualization; Methodology; Investigation; Writing. MS: Conceptualization; Visualization; Writing—review and editing and discussion. MG: Methodology and Editing MG: Synthesis SP: Synthesis; Formal analysis.

Declarations

Consent to Participate Not applicable.

Consent for Publication Not applicable.

Conflict of Interest The authors declare that they have no conflicts of interest.

References

1. Machado SWM, Santana JC, Pedrosa AMG, Souza MJB, Coriolano ACF, Morais EKL (2018) Catalytic cracking of isopropylbenzene over hybrid HZSM-12/M41S (M41S = MCM-41 or MCM-48) micro-mesoporous materials. Pet Sci Technol 36: 923–929. https://doi.org/10.1080/10916466.2018.1454950
2. Ryoo R, Kim JM, Ko CH, Shin CH (1996) Disordered molecular sieve with branched mesoporous channel network. J Phys Chem 100:17718–17721. https://doi.org/10.1021/jp9620835
3. Gholamzadeh P, Mohammadi Ziarani G, Badiei A (2017) ***Immobilization of lipases onto the*** SBA-15 ***mesoporous silica***. Biocatal Biotransfor 35:131–150. https://doi.org/10.1080/10242422.2017.1308495
4. Alothman ZAA (2012) Review: fundamental aspects of silicate mesoporous materials. Materials. 5:2874–2902. https://doi.org/10.3390/ma5122874
5. Li Z, Zhang Y, Feng N (2019) Mesoporous silica nanoparticles: synthesis, classification, drug loading, pharmacokinetics, biocompatibility, and application in drug delivery. Expert Opin Drug Deliv 16:219–237. https://doi.org/10.1080/17425247.2019.1575806
6. Sanaeishoar H, Sabbaghan M, Mohave F (2015) Synthesis and characterization of micro-mesoporous MCM-41 using various ionic liquids as co-templates. Micropor Mesopor Mat 217:219–224. https://doi.org/10.1016/j.micromeso.2015.06.027
7. Liu L, Xiong G, Wang X, Cheng X (2011) Synthesis of Nanosized AlKIT-1 mesoporous molecular sieve and its catalytic performance for the conversion of 1,2,4-Trimethylbenzene. Catal Lett 141: 1136–1140. https://doi.org/10.1007/s10562-011-0580-8
8. Roto R, Kartini I, Motuzas J, Triyana K, Siswanta D, Dwi Wahyuningsih T, Kusumaatmaja A (2019) Rapid synthesis of MCM-41 from Rice husk using ultrasonic wave: Optimation of sonication time. Mater Sci Forum 948:198–205. https://doi.org/10.4028/www.scientific.net/MSF.948.198
9. Coutino-Gonzalez E, Manriquez J, Robles I, Espejel-Ayala F (2018) Synthesis of MCM-41 material from acid mud generated in the aluminum extraction of kaolinite mineral. Enviro Prog Sustain Energy doi: 101002/ep13069
10. Loganathan S, Kumar K, Ghoshal AK (2019) Fabrication of mesoporous silica MCM-41 via sol-gel and hydrothermal methods for amine grafting and CO_2 capture application. Urban Ecology, Water Quality and Climate Change 38:341–349. https://doi.org/10.1007/978-3-319-74494-0_26
11. Azizi SN, Ghasemi S, Rangriz-Rostami O (2018) Synthesis of MCM-41 nanoparticles from stem of common reed ash silica and their application as substrate in electrooxidation of methanol. Bull. Mater. Sci 88:1–13. https://doi.org/10.1007/s12034-018-1580-8
12. Ryoo R, Kim JM, Shin CH, Lee JY (1997) Synthesis and hydrothermal stability of a disordered mesoporous molecular sieve. Stud Surf Sci Catal 105:45–52. https://doi.org/10.1016/S0167-2991(97)80537-X
13. Taubert A. (2016) Inorganic nanomaterials synthesis using ionic liquids, Encyclopedia of Inorganic and Bioinorganic Chemistry, 1–14 doi: https://doi.org/10.1002/9781119951438.eibc0355.pub2
14. Li RX (2004) Green solvents: synthesis and application of ionic liquids. Chemistry Technology Press, Beijing
15. Isambert N, Duque MMS, Plaquevent JC, Genisson Y, Rodriguez J, Constantieux T (2011) Multicomponent reactions and ionic liquids: a perfect synergy for eco-compatible heterocyclic synthesis. Chem Soc Rev 40:1347–1357. https://doi.org/10.1039/C0CS00013B
16. Sanaeishoar H, Sabbaghan M, Mohave F, Nazarpour R (2016) Disordered mesoporous KIT-1 synthesized by DABCO-based ionic liquid and its characterization. Micropor. Mesopor. Mat. 228: 305–309. https://doi.org/10.1016/j.micromeso.2016.04.003
17. Barrett EP, Joyne LG, Halenda PP (1951) The determination of pore volume and area distributions in porous substances. I. Computations from nitrogen isotherms. J. Am. Chem. Soc. 73: 373–380. https://doi.org/10.1021/ja01145a126
18. Yue Y, Sun Y, Gao Z (1997) Disordered mesoporous KIT-1 as a support for hydrodesulfurization catalysts. Catal Lett 47:167–171. https://doi.org/10.1023/A:1019084400340
19. Gregg SJ, Sing KSW (11997) adsorption, Surface Area and Porosity; Academic: London
20. Chen LJ, Xu WH, Zhang JD, Holmes MA, Morris J (2011) Syntheses of complex mesoporous silicas using mixtures of non-ionic block copolymer surfactants: understanding formation of different structures using solubility parameters. Colloid Interface Sci 353:169–180. https://doi.org/10.1016/j.jcis.2010.09.043
21. Wei J, Yue Q, Sun Z, Deng Y, Zhao D (2012) Synthesis of dual-mesoporous silica using non-ionic diblock copolymer and cationic surfactant as co-templates. Angew Chem Int Ed 51:6149–6153. https://doi.org/10.1002/anie.201202232
22. Wali LA, Khulood KH, Alwan AM (2019) Rapid and highly efficient detection of ultra-low concentration of penicillin G by gold nanoparticles/porous silicon SERS active substrate. Spectrochim Acta A Mol Biomol Spectrosc 206:31–36. https://doi.org/10.1016/j.saa.2018.07.103
23. Wang T, Kaper H, Antonietti M, Smarsly B (2007) Templating behavior of a long-chain ionic liquid in the hydrothermal synthesis of mesoporous silica. Langmuir 23:1489–1495. https://doi.org/10.1021/la062470y